STUDY OF BIOLOGICAL SYSTEMS BY HIGH-RESOLUTION EPR IN THE 2 mm RANGE (REVIEW)

V. I. Krinichnyi

UDC 543.42:541.64

For investigation of the structure and dynamics of biological systems, various methods are used which are based on the "label" or "probe" principle: the luminescent label method [1], the Mössbauer method [2], the method involving dissipation of electrons in electron-dense groups of atoms [3]. The most widely used method for these purposes is the spin label and spin probe method, first proposed by McConnell more than twenty years ago [4] and based on introduction of nitroxide radicals into the biological system [4-7]. The parameters of the EPR spectra of the radicals depend on the polarity, structure, and dynamics of the microenvironment at their localization site. Therefore introduction of spin labels and probes into different sections of enzymes, nucleic acids, and membranes allows us to establish the polarity and mobility profile for the studied systems and to study their topography.

Most often, such studies are carried out in the 3 cm EPR range (X-band EPR). However, in this wavelength range, the EPR spectra of organic free radicals are recorded in a narrow interval of magnetic field values. This leads to weak resolution of multicomponent EPR spectra and hinders the use of the method for establishment of the structure and dynamics of the microenvironment of the radical in biological systems.

Thus from the 3 cm EPR spectra, it could not be unambiguously determined whether the relaxation changes in the spectrum are due to anisotropic motion of the radical in the low-frequency region ($\nu \approx 10^7$-$5 \cdot 10^8$ sec^{-1}) [4] or to fast rotation of its nitroxide fragment with frequency $\nu \approx 10^9$ sec^{-1} in a limited cone [8]. Additional difficulties arise when recording several paramagnetic centers in this EPR range with close magnetic parameters, and also when determining the micropolarity or their environment in biological systems [6].

Thus when studying biological systems in the 3 cm range, substantial limitations are imposed on the EPR method.

In some cases, an increase in the accuracy of the method is realized when using the modulation-free method for recording the EPR spectra [9]. Slow molecular motions in the frequency region $\nu \leq 10^7$ sec^{-1} can be registered using the microwave saturation transfer method [5, 10]. The information content of the EPR spectra can be increased by deutero-substitution of the protons in the radical and the molecules of the medium, for which the contribution from unresolved hyperfine structure (hfs) of these nuclei to the width of individual components in the spectrum decreases [11].

However, a more general method for increasing the accuracy and information content of the method is to go to the millimeter EPR range [5, 12-16]. In this range, the absolute sensitivity and spectral resolution are significantly increased when registering polyoriented paramagnetic centers in model systems.

In this paper, we generalize the first results from an investigation of the structural and dynamic characteristics of a whole series of biological specimens (proteins, enzymes, membranes, micelles, biopolymers) by the high-resolution EPR method in the 2 mm range. We have demonstrated the possibility in principle of making a detailed study of anisotropic ultraslow motions using the method of microwave saturation transfer and the possibility of identifying peroxide radicals in biological systems from the 2 mm EPR spectra.

PHYSICAL PRINCIPLES OF THE METHOD

The paramagnetic properties of organic radicals are due to the intrinsic angular momentum of the unpaired electron. In an external magnetic field, the magnetic moments of the elec-

Institute of Chemical Physics, Academy of Sciences of the USSR, Chernogolovka Branch, Moscow Region. Translated from Zhurnal Prikladnoi Spektroskopii, Vol. 52, No. 6, pp. 887-905, June, 1990. Original article submitted May 22, 1989.

0021-9037/90/5206-0575 $12.50

trons can be oriented either in the direction of the field or opposite to the direction of the field. Subsequent superposition of electromagnetic radiation on this electronic system leads to its resonance absorption when the following condition is satisfied:

$$h\nu = g\beta H, \tag{1}$$

where h is Planck's constant; ν is the frequency of the electromagnetic radiation; g is the Landé factor; β is the Bohr magneton; H is the strength of the external magnetic field.

The unpaired electron in the nitroxide radical occupies the antibonding π^*-orbital formed by the p orbitals of the nitrogen and oxygen atoms. Interaction of the electron with the nonzero nuclear spin of the nitrogen atom leads to the appearance of hyperfine structure in its EPR spectrum. The molecular orbitals of the radical are rigidly fixed and oriented. This determines the tensor character of the hyperfine coupling and its g factor. The axes of the magnetic tensors of the radical coincide and are oriented as follows: the X axis – along the direction of the NO bond; the Z axis – in the plane of the π bond of the NO fragment; the Y axis is perpendicular to the X and Z axes.

The structural and dynamic properties of its microenvironment exert a substantial effect on the magnetic parameters of the nitroxide radicals.

In biological systems, the nitroxide radicals can be formed with their own microenvironment of donor–acceptor, electrostatic, and other complexes [17]. In the first case, about 1% of the spin density is transferred to the ligand by means of the collective hydrogen bond, which is responsible for the interaction of the unpaired electron with the ligand protons. The magnetic parameters of such a complex will be determined by the donor–acceptor properties of the ligand substituents. In electrostatic complexes, the determining factor is the interaction of the dipole of the radical and the fragments of the biosystem surrounding it; this leads to a corresponding perturbation of the Hückel molecular orbitals and the Coulomb integrals of the NO fragment. In electrostatic complexes, the change in the A_{ZZ} value of the hfs tensor will depend on the properties of the fragments of the environment [18]:

$$\delta A_{ZZ} = B\frac{\mu_L \rho_L}{M_L}, \tag{2}$$

where $B = 22er\frac{kT\mu_R}{\beta}$ (e is the charge on the electron, r is the radius of the NO fragment, β is the resonance integral of the C–C bond, k is the Boltzmann constant, T is the temperature, μ_R is the dipole moment of the radical); ρ_L, M_L, μ_L are respectively the effective density, the molecular mass, and the dipole moment of the fragments of the environment.

In formation of the complexes, a shift of the $n-\pi^*$ band also occurs in their electronic absorption spectra. This is evidence for a change in the energy of the transition from the n to the π^*-orbital. And complexation of the radical with an electron-acceptor ligand leads to lowering of the n-orbital, and complexation with an electron-donor ligand leads to lowering of the π^*-orbital. In this case, the g_{XX} value of the g tensor changes most strongly [19].

Thus with an increase in polarity of the microenvironment of the nitroxide radical, simultaneous increase in the A_{ZZ} value and decrease in the g_{XX} value of the radical complex should occur [19]. Since in biological specimens the radical can interact with different types of fragments, in its EPR spectrum we can observe inhomogeneous broadening and even splitting of the individual components.

With a decrease in viscosity in biological systems, freezing out of molecular motions occurs. This leads to broadening of the components of the g and A tensors (depending on the model for the motion: Brownian diffusion, jump reorientation) of the radical introduced into the system [20]. Relaxation changes in the EPR spectrum of randomly oriented spin-labeled systems will not be apparent for the part of the systems in which the radicals are oriented with the preferred axis of rotation along the direction of the external magnetic field.

Thus, for a radical with preferred rotation about the molecular X axis, upon freezing out of the motion the relaxation changes are apparent first of all for the Y and Z components of the EPR spectrum. Upon further decrease in the viscosity, the X component of the EPR spectrum is also included in the motion.

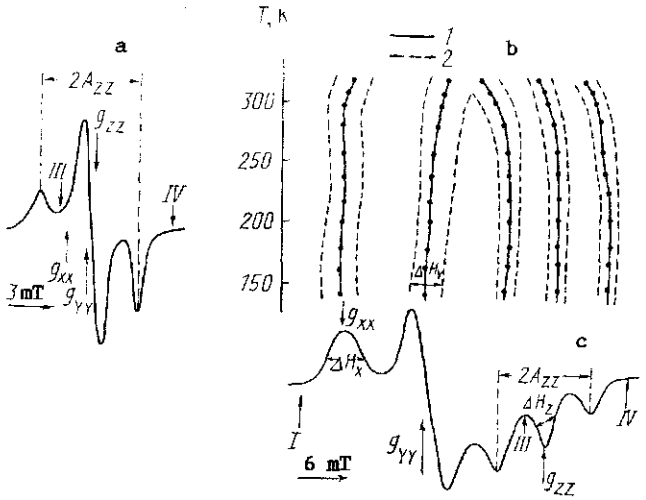

Fig. 1. EPR spectra of radical I in lyophilized egg lysozyme, registered at T = 160 K in the 3 cm (a) and 2 mm (c) EPR ranges and the change in the positions (1) and widths (2) of the components of the 2 mm EPR spectrum vs. temperature (b). I, III, IV are the components of the reference (Mn^{2+}). The measured components of the magnetic parameters are shown.

Relaxation changes are apparent both in the shift and in the broadening of individual components of the EPR spectrum. The magnitude of such broadening is inversely proportional to the residence time of the X-anisotropic radical in the corresponding orientation relative to the direction of the external magnetic field [15]

$$\gamma \cdot \delta H_X \simeq 2\nu_\perp; \quad \gamma \cdot \delta H_Y = \gamma \cdot \delta H_Z \simeq \nu_\parallel + \nu_\perp, \tag{3}$$

where γ is the gyromagnetic ratio; δH_i is the broadening of the corresponding components of the EPR spectrum; $\nu_\parallel$ and $\nu_\perp$ are the frequencies corresponding to the residence time of the radical in respectively the parallel and perpendicular orientations relative to the external magnetic field.

Analogously, we can determine the broadening of the components of the EPR spectrum of the radical with other axes of preferred rotation.

Thus, in order to study the fine features of the structure and dynamics of biological spin-labeled systems, we need to register all the components of their magnetic parameters.

According to relation (1), the spectral resolution of the components of the EPR spectrum of paramagnetic centers with an anisotropic g factor is proportional to the magnitude of the applied magnetic field. Therefore, in the EPR spectrum of spin-labeled egg lysozyme, registered in the 3 cm EPR range (Fig. 1a), we observe virtually complete superposition of the canonical components of the spectrum.

In the 2 mm EPR range, the EPR spectrum of the indicated system is more informative (Fig. 1c). In this range, complete spectral resolution of the components of the g tensor of the spin label occurs. This makes it possible to determine all the components of its magnetic parameters with high accuracy.

The increase in the spectral resolution also proves to be important in the study of other organic radicals, including peroxy radicals.

EXPERIMENTAL

The EPR spectra of spin-labeled biological systems and radicals in different matrices were recorded using a 2 mm EPR spectrometer with a superconducting solenoid and reflective resonator of the H_{011} type [21]. Its absolute sensitivity with respect to a point sample is $5 \cdot 10^8$ spins/mT and its concentration sensitivity with respect to an aqueous sample is $6 \cdot 10^{13}$ spins/mT·cm^3.

The g factor was calibrated using Mn^{2+} as the reference. The second-order correction to the effective field [22] for this reference in the 2 mm EPR range is 65 μT (in the 3 cm EPR range, it is greater than 1 mT) and does not introduce substantial error into determination of the magnetic parameters of paramagnetic centers.

As the spin labels and probes, in this work we used the following nitroxide radicals:

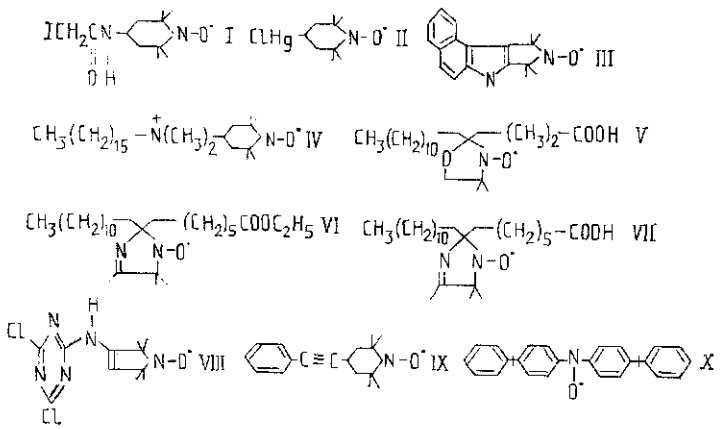

The samples were quartz capillaries with outer diameter 0.6 mm and length 6 mm, filled with the appropriate spin-labeled system.

The magnetic parameters of the indicated radicals in different biological and model systems, determined from the EPR spectra at temperatures for which all the motions in them were frozen, are presented in Table 1.

STRUCTURE OF THE MICROENVIRONMENT AND MOLECULAR MOBILITY OF NITROXIDE RADICALS IN BIOLOGICAL SYSTEMS

As was shown above, the parameters most sensitive to the change in polarity and structure of the microenvironment of radicals are the g_{XX} and A_{ZZ} values. Therefore in order to determine the properties of the microenvironment of the radicals in biological and model systems, we used the correlation dependence of these parameters.

Egg Lysozyme. In [23] we studied egg lysozyme preparations, modified by spin label 1 at the hist-15 group according to the technique outlined in [24].

The EPR spectrum of the lyophilized frozen sample is characterized by significant inhomogeneous broadening of individual components, which is partially removed upon saturation of the sample with water (Fig. 1c). This fact is evidence for interaction of the label with the hydroxyl fragments of the protein of different structures.

In Fig. 2, we present the magnetic parameters of radical I in frozen organic solvents of different polarities and in lysozome with relative humidity 0.04-0.96. From the figure it is obvious that an increase in the polarity of the microenvironment of radical I in model systems leads to a monotonic decrease in the g_{XX} value and an increase in the A_{ZZ} value. This is unambiguous evidence for formation of a n–σ-radical complex with the molecules of the environment in these systems [17]. Such a complex forms a radical in lysozyme. The different correlation dependences of g_{XX}–A_{ZZ} in the model systems and in lysozyme with different relative humidities allows us to conclude that there is a change in the conformation of the radical ring in the latter case under the action of the protein environment. The closeness of the magnetic parameters of the frozen lyophilized spin-labeled lysozyme and the radical solution in n-butanol indicates a similarity in polarity and structure of the microenvironment of the radical fragment in these systems.

In the EPR spectra of spin-labeled samples of lysozyme with relative humidity less than 0.8 in the temperature interval 130-320 K we did not note relaxation changes in the line shape. This may be evidence for rigid fixation of the radical fragment close to the hydrogen-containing groups in these samples.

Heating the water-saturated sample leads to appreciable broadening and field shift of the individual components of its EPR spectrum (Fig. 1b). In the temperature interval 130-200 K we observe narrowing of the X component of the EPR spectrum, which can apparently be

TABLE 1. Magnetic Parameters of Nitroxide Radicals I-X in Frozen Biological and Model Systems

Matrix	R	g_{XX}	g_{YY}	g_{ZZ}	giso	A_{ZZ}, mT
			I			
Toluene	—	2,00953	2,00577	2,00176	2,00569	3,40
iso-Butanol	—	2,01010				
		2,00935	2,00602	2,00197	2,00578	3,50
Ethanol	—	2,00910	2,00573	2,00210	2,00564	3,58
Ethanol + water	0,25	2,00902	2,00543	2,00212	2,00552	3,60
Ethanol + water	0,50	2,00890	2,00602	2,00214	2,00569	3,65
Ethanol + water	0,66	2,00883	2,00608	2,00201	2,00564	3,70
Methanol	—	2,00860	2,00550	2,00178	2,00529	3,73
Water + glycerin	0,92	2,00834	2,00571	2,00167	2,00524	3,77
Lysozyme	0,04	2,00946	2,00646	2,00217	2,00603	3,50
Lysozyme	0,35	2,00923	2,00617	2,00220	2,00587	3,61
Lysozyme	0,60	2,00912	2,00614	2,00214	2,00580	3,69
Lysozyme	0,80	2,00908	2,00603	2,00211	2,00574	3,74
Lysozyme	0,96	2,00902	2,00624	2,00211	2,00579	3,85
HSA	0,04	2,00893	2,00585	2,00164	2,00547	3,60
HSA	0,96	2,00842	2,00570	2,00170	2,00527	3,75
α-Chymotrypsin	0,04	2,00912	2,00598	2,00210	2,00573	3,58
α-Chymotrypsin	0,66	2,00839	2,00613	2,00219	2,00557	3,67
			II			
HSA	0,04	2,00998				
		2,00883	2,00612	2,00216	2,00570	3,64
HSA	0,96	2,00863	2,00613	2,00215	2,00563	3,84
			III			
HSA	0,04	2,00855	2,00621	2,00214	2,00563	3,55
HSA	0,96	2,00845	2,00614	2,00210	2,00556	3,67
			IV			
Membranes	—	2,00980	2,00642	2,00232	2,00618	3,67
			V			
Membranes	—	2,00918	2,00614	2,00230	2,00587	3,50
			VI			
Ethanol	—	2,01044				
		2,00984	2,00696	2,00302	2,00661	3,39
			VII			
Octane	—	2,00951	2,00611	2,00215	2,00592	3,28
n-Propanol	—	2,00955				
		2,00894	2,00619	2,00217	2,00597	3,29
Ethanol	—	2,00901	2,00617	2,00219	2,00597	3,30
Methanol	—	2,00882	2,00626	2,00228	2,00579	3,61
Micelles w/o protein	2,5	2,00952	2,00626	2,00226	2,00601	3,41
»	5,5	2,00946	2,00614	2,00213	2,00591	3,32
Micelles with protein	3	2,00954	2,00622	2,00221	2,00599	3,34
α-Chymotrypsin	6	2,00958	2,00622	2,00231	2,00603	3,41
»	10	2,00950	2,00618	2,00215	2,00594	3,36
»	15	2,00954	2,00622	2,00220	2,00599	3,41
»	20	2,00950	2,00622	2,00239	2,00601	3,36
»	30	2,00946	2,00621	2,00222	2,00597	3,41
»	40	2,00939	2,00618	2,00217	2,00591	3,32
»	50	2,00943	2,00614	2,00217	2,00591	3,32
»	60	2,00946	2,00622	2,00226	2,00598	3,35
»	80	2,00937	2,00607	2,00210	2,00585	3,34
			VIII			
Octane	—	2,00872	2,00633	2,00214	2,00573	3,43
Ethanol	—	2,00865	2,00622	2,00221	2,00569	3,52
Methanol	—	2,00857	2,00617	2,00209	2,00560	3,69
			VIII			
Water + glycerin	0,90	2,00840	2,00627	2,00215	2,00561	3,81
Cotton "5595-V"	0,04	2,00842	2,00592	2,00224	2,00553	3,76
Cotton "Tashkent-I"	0,04	2,00863	2,00622	2,00232	2,00572	3,55
Cotton "Tashkent-I" + wilt	0,04	2,00840	2,00562	2,00212	2,00538	3,35
Cellulose (Ts)	0,04	2,00762	2,00582	2,00211	2,00518	3,37
Cellulose (TsA-I)	0,04	2,00791	2,00584	2,00222	2,00532	3,57
Cellulose (TsA-II)	0,04	2,00783	2,00574	2,00227	2,00528	3,49

Table 1 (continued)

Matrix	R	g_{XX}	g_{YY}	g_{ZZ}	g_{iso}	A_{ZZ}, mT
			1X			
tert-Butylbenzene	—	2,00979	2,00622	2,00206	2,00602	3,41
			X			
tert-Butylbenzene	—	2,00947	2,00541	2,00217	2,00568	3,21

Note. Errors in measurement of the components of the g and A tensors are $7 \cdot 10^{-5}$ and $3 \cdot 10^{-2}$ mT, respectively. R is the relative water content (in model systems), degree of hydration (in micelles), relative humidity (in other biological systems). In the case when there is splitting of the X component of the EPR spectrum, in the calculation of g_{iso} we considered the low-field X component of the EPR spectrum.

explained by averaging of the unresolved hyperfine structure of the protons in the radical and the protein fragments. This fact is evidence for an effect of humidification on the molecular motions in the sample even at T < 200 K. When T > 250 K, the X component of the EPR spectrum is shifted downfield (Fig. 1b). This cannot be explained by freezing out the molecular motions. Since such an effect is missing in the lyophilized sample, it can be assigned to weakening of the hydrogen bond of the NO fragment with the surrounding radical by the water molecules upon heating.

Relaxation changes in the rest of the components of the EPR spectrum of the water-saturated sample are registered from T = 260 K and are described in terms of anisotropic rotational diffusion. Starting from this temperature, apparently weakening of the bond of the NO fragment of the radical with the surface protein groups occurs, as well as subsequent hydration of the radical and protein groups. The water molecules thus play the role of a specific plasticizer of the mobility of the protein globule and the radical.

As was shown above, upon anisotropic rotation of the radical, the components of its EPR spectrum will broaden and shift with respect to the field in different ways. In the EPR spectrum of spin-labeled lysozyme with relative humidity 0.96, upon heating the Y component is broadened most strongly, which is evidence for slight anisotropy of rotation of the radical about the Z axis in this sample. Theoretical calculations [23] confirmed this hypothesis.

The nitroxide fragment of the label is located 1.1 nm from the NH group his-15 and 1.0-1.1 nm from the protons phe-3, val-92, and iso-88 [25]. This corresponds to a prolate conformation of the label and localization of its nitroxide fragment in the region of the notch formed by the indicated hydrophobic groups. The mobility of the nitroxide fragment remains low all the way up to T = 305 K with $\tau_c \geq 5 \cdot 10^{-8}$ sec ($\tau_\perp \geq 1.1 \cdot 10^{-7}$ sec) $\tau_\parallel \geq 2.2 \cdot 10^{-8}$ sec) and is apparently realized about the C–NH- and $-CH_2CO$-bonds. The motion is restricted by interaction of the radical with the protein groups, possibly with the molecules of "viscous" water close to the surface of the protein, and reflects the effective microviscosity of the water–protein matrix in the given region. The coefficient of effective local viscosity in the hydrophobic pocket of the lysozyme, calculated at T = 300 K using the Stokes–Einstein formula, was $\eta \approx 60$ Pa·sec.

Human Serum Albumin. In [26], a sample of human serum albumin (HSA) was studied, labeled at the SH group with radicals I and II, and also with probe III introduced according to the technique outlined in [27].

In Fig. 2, we present the magnetic parameters of human serum albumin, modified by radicals I-III, with relative humidity 0.04 and 0.96. From the figure it is obvious that the magnetic parameters of HSA with labels I and II and relative humidity 0.04 fall on the g_{XX}–A_{ZZ} correlation curve for the model systems. This may be evidence for generation of a n–σ radical complex in HSA with molecules of the environment, and also for the similar structure and polarity of the microenvironment at the localization site of these labels in lyophilized HSA and in the frozen ethanol system.

Upon saturation of the protein with water, the radical fragment of label I is solvated with its molecules similar to the way it is solvated in a water–glycerin mixture. Such ac-

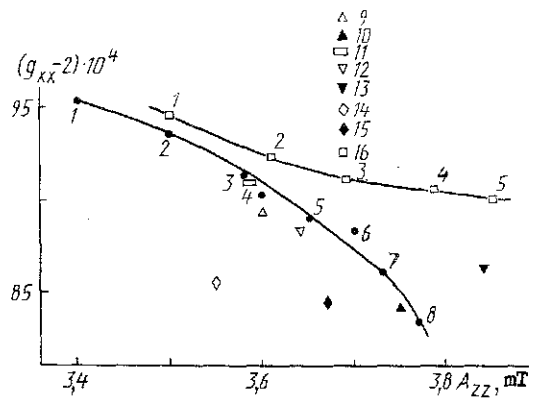

Fig. 2

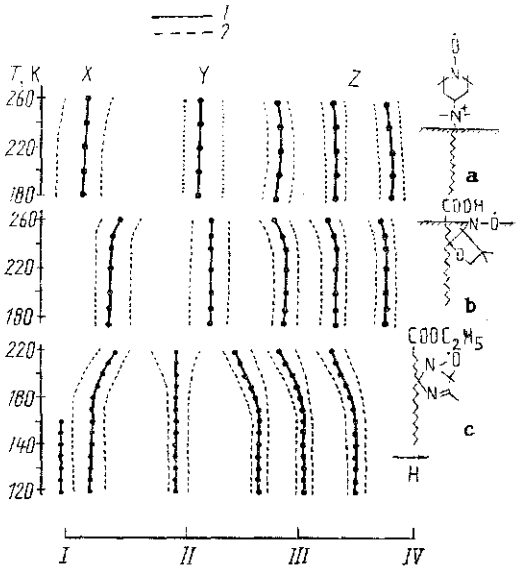

Fig. 3

Fig. 2. Correlation dependence of $g_{XX}-A_{ZZ}$ for radical I in frozen (T = 140 K) toluene (1), isobutanol (2), ethanol (3), water–ethanol matrix with relative water content 0.25 (4), 0.50 (5), 0.66 (6), methanol (7), water–glycerin matrix (8), egg lysozyme (16) with relative humidity 0.04 (1), 0.35 (2), 0.60 (3), 0.80 (4), 0.96 (5), human serum albumin with relative humidity 0.04 (9), 0.96 (10), α-chymotrypsin with relative humidity 0.04 (11), for radicals II (12, 13) and III (14, 15) in human serum albumin with relative humidity 0.04 and 0.96, respectively.

Fig. 3. Change in the positions (1) and widths (2) of components of the EPR spectra of radicals IV (a), V (b) in liposomal membranes, and VI (c) in ethanol vs. temperature. I–IV) position of the Mn^{2+} components.

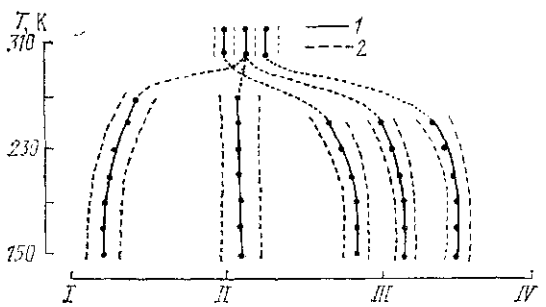

Fig. 4. Change in the positions (1) and widths (2) of components of the EPR spectrum of radical VII in inverted micelles with the protein α-chymotrypsin vs. temperature. I-IV) position of the components of the reference Mn^{2+}.

cessibility of the radical fragment to the aqueous environment in HSA is also characteristic for other radicals. However, the nature of the interaction of the nitroxide fragments of radicals with different structures in water-saturated HSA is different (see Fig. 2).

The EPR spectrum of HSA, modified by label II, contains a split X component, which indicates the existence of different radical complexes in this system.

Liposomal Membranes. In the realization of important biochemical and biophysical processes in which bilayer membranes participate, an exceptionally important role is played by their conformational and molecular dynamic properties.

In [28], a comparison is made between the mobility of probes IV and V introduced into the liposomes, and also probe VI in an ethanol matrix.

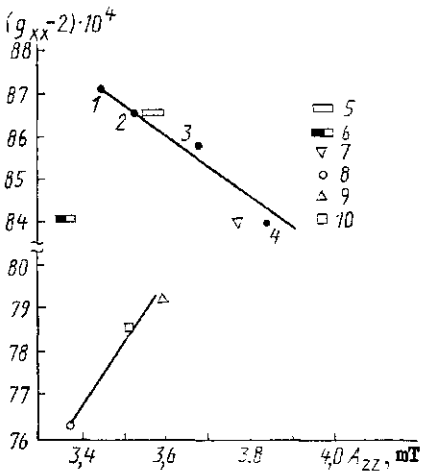

Fig. 5

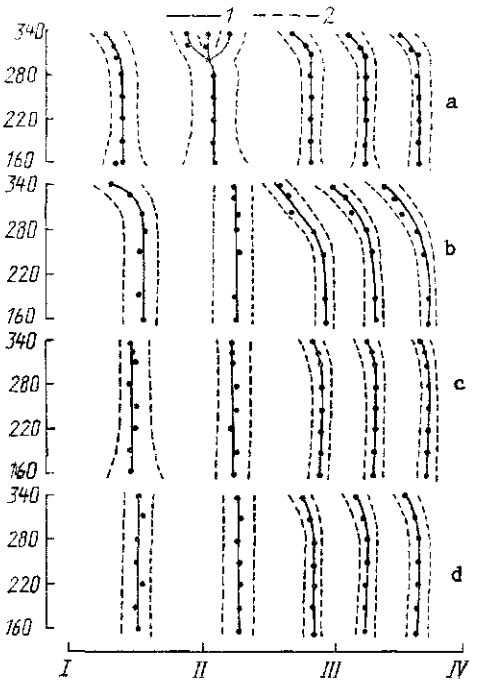

Fig. 6

Fig. 5. Correlation dependence of g_{XX}—A_{ZZ} for radical VIII in frozen (T = 150 K) octane (1), ethanol (2), methanol (3), water—glycerin matrix (4), cotton fibers "Tashkent-I" (5), "Tashkent-I" + wilt (6), 5595-V (7), cellulose samples Ts (8), TsA—I (9), TsA-II (10) with relative humidity 0.04.

Fig. 6. Change in the positions (1) and widths (2) of components of the EPR spectra of radical VIII in 5595-V cotton fibers (a) and cellulose samples Ts (b), TsA-I (c), and TsA-II (d) vs. temperature. I-IV) components for the reference Mn^{2+}.

The EPR spectra of liposomal membranes with introduced probes at T = 180 K differ little in shape from the EPR spectrum of the frozen model system. In the latter, at $T \leq 160$ K we register splitting of the X component of the EPR spectrum, which can be apparently explained by the presence of different radical complexes in it.

Upon heating, in the EPR spectra of modified liposomal membranes we observe relaxation changes in the line shape. The change in the width and position with respect to field of individual components of the EPR spectra of the studied systems vs. temperature is presented in Fig. 3.

From the figure it is obvious that for radical VI in an ethanol matrix for T > 150 K, isotropic rotation is characteristic. A different character for the change in the line shape is observed for membrane systems (Fig. 3a, b). The major differences from the model system (not considering the shift toward higher temperatures and the lesser degree of the registered changes) involve the fact that in their EPR spectra, we observe a shift with respect to field of the X and Z components with an increase in temperature with very insignificant broadening. Such differences can be explained by the slight anisotropic rotation of the radicals about their own Y axis of some compensation of the broadening by the effect of line narrowing as a result of the decrease in the contribution to their width from the unresolved hyperfine structure of the surrounding protons. The rotational correlation time of the probes in liposomal membranes was estimated within the Brownian diffusion model and was $\tau_c \approx 10^{-7}$ sec at T = 260 K.

Relaxation changes in the EPR spectra of probe IV in the membranes are registered for $T \geq 200$ K. Analogous changes in the EPR spectra of probe V in the membranes are apparent at higher temperatures ($T \geq 240$ K), but they demonstrate a sharper temperature dependence. These differences can be explained assuming that the positively charged nitroxide fragment of probe IV is localized on the surface polar sections (accessible to water) of the liposomal membrane [28], while the NO fragment of probe V is located in its lipid part [29].

The observed changes in the line shape are complicated in character, and apparently a single parameter is sufficient to describe them: the correlation time. At the qualitative level, however, we can conclude that the rotational frequency of the probes in the membranes at T = 260 K is not greater than $\nu \approx 10^7$ sec^{-1}, and the nature of the dependence of these motions on temperature is mainly determined by the immediate environment of the probe. Thus for probe IV, localized in the surface layers of the membrane, the increase in the mobility for T > 200 K is apparently connected with melting of the surface water. The active fragment of probe V is found in the relatively more rigid lipid part of the membrane, adjacent to the surface layers. Therefore, freezing out of its molecular mobility occurs with a higher temperature coefficient.

Comparison of the magnetic parameters, modified by probe V, for the membranes and model systems with radicals similar in structure allowed us to hypothesize that the structure and polarity of the microenvironment of probe V in the liposomal membranes and probe VII in the frozen methanol matrix are similar.

Inverted Micelles. Solutions of surfactants in organic solvents have been considered as prospective systems for accomplishment of different biochemical processes [30]. Owing to the polar core, inverted micelles acquire the ability for solubilization of different ions and polar substances, including water molecules. The catalytic activity of the protein included in their inner cavity depends substantially on the polarity and structure of the protein environment. Therefore, the spin label and spin probe method is widely used in order to study inverted micelle–protein systems [6, 31, 32].

Below we present the results of investigation of the polarity of the microenvironment and the dynamic properties of paramagnetic probe VII in the shell of inverted micelles of sodium diisooctylsulfosuccinate in octane containing the solubilized protein α-chymotrypsin, and also label I in this protein in the two-millimeter EPR range [33].

From comparison of magnetic parameters for micellar and model systems (see Table 1), it is obvious that probe VII in the shell of the micelles has a virtually nonpolar environment, and its magnetic parameters weakly depend on the degree of hydration, R = $[H_2O]/[Surf]$. Consequently, the radical fragment is localized in the hydrophobic zone of the micelle shell and does not come into direct contact with the water molecules within it. The insignificant changes in the magnetic parameters of the probe with a change in the composition of the micelle–protein system can be explained by the effect of the degree of hydration on the dimensions and general state of the micellar shell. The data obtained do not confirm the conclusions drawn in [31], in which anomalously low A_{ZZ} values for probe VII in hydrated micelles are explained by several localization sites for it.

With an increase in temperature above 200 K, the components of the EPR spectra of the studied systems are broadened and shifted with respect to field as a consequence of freezing out the molecular motions (Fig. 4). At T = 260 K, complete coalescence of the components of the EPR spectra occur into a broad (2 mT) singlet, corresponding to a radical with correlation time $\tau_{C_1} \approx 10^{-8}$ sec. A practically isotropic triplet corresponding to the more frozen radical, $\tau_{C_2} \approx 10^{-10}$ sec, is superimposed on this singlet (Fig. 4). This indicates that about 4% of the probes are found outside the lipid layer and in this case have higher mobility and come in contact with the water molecules solubilized in the inner cavity of the micelles. The difference in the g factors of the radicals with different rotational frequencies indicates a change in the conformation of the microenvironment of the probe when it goes from the shell to the inner cavity of the micelles, and a variation in the degree of hydration.

Comparison of the experimentally obtained and theoretically calculated EPR spectra showed that addition of protein to the micellar system leads to more than two-fold decrease in the activation energy for rotation of the probe [33]. This is evidence for the structure of the micelles becoming more rigid in such a transition. The reverse effect is observed with an increase in the degree of hydration of the micelle–protein system.

The magnetic parameters of α-chymotrypsin with relative humidity 0.04, modified by label I at the methionine-192 group in the region of the active center, fall on the g_{XX}–A_{ZZ} correlation line for the model systems (Fig. 2). As was the case for human serum albumin, this can be evidence that the structure and polarity of the microenvironments for this label are similar in α-chymotrypsin and in the frozen ethanol solution.

In the EPR spectrum of lyophilized spin-labeled α-chymotrypsin, all the way up to T = 300 K we did not note any relaxation changes in the line shape due to the rigid fixation of

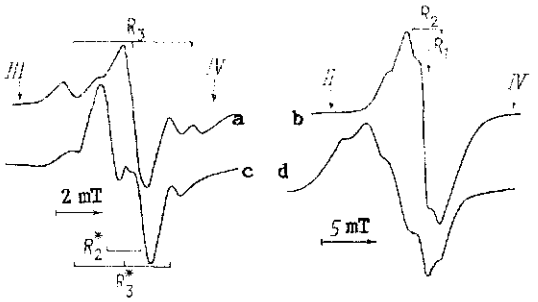

Fig. 7. EPR spectra of γ-irradiated (dose 10 MRad) cellulose samples Ts (a, b) and TsA-II (c, d), recorded at T = 290 K in the 3 cm (a, c) and 2 mm (b, d) EPR ranges. II-IV) components of the reference Mn^{2+}.

the radical fragment by its microenvironment. In the temperature interval 220-260 K, the X component of the EPR spectrum is reversibly shifted upfield, apparently due to the change in the conformation of the microenvironment of the radical.

Above 300 K, the components of the EPR spectrum of spin-labeled α-chymotrypsin are appreciably broadened and shifted toward the center of gravity of the spectrum. The correlation time, activation energy for rotation of the radical, and the effective microviscosity at its localization site, calculated from the EPR spectrum, at T = 310 K, were respectively, $1.8 \cdot 10^{-7}$ sec, 80 ± 8 kJ/mole, and 22 Pa·sec. The motions of the radical are no longer restrained when the spin-labeled α-chymotrypsin is placed into a micelle with degree of hydration six ($\tau_c \approx 5.5 \cdot 10^{-11}$ sec) [31].

The data obtained indicate the cooperative effect of water and bioglobules on the structure of the micelle, the microenvironment, and the mobility of the probe far from the interfacial surface and the labels localized in the region of the active center of α-chymotrypsin.

Cotton Fibers and Cellulose. In order to establish the mechanism of biochemical conversions occurring in cotton fibers and cellulose, we need information about the structural and dynamic properties of these natural biopolymers. For this purpose EPR spectroscopy has been widely used [34, 35]. However, as in the preceding cases, the insufficient spectral resolution in the 3 cm EPR range does not allow us to establish a sufficiently complete picture for the processes occurring in these systems.

The high-resolution EPR method has been used to study different parameters of modified cotton fibers [36] and microcrystalline cellulose [37].

We investigated cotton fibers obtained from 5595-V and "Tashkent-I" plants, and also microcrystalline cellulose (Ts), amorphicized by a pressure of $2 \cdot 10^9$ Pa between Bridgman anvils with shear 10 and 400° (TsA-I and TsA-II respectively). The modification of the cotton fibers and cellulose by radical VIII was done according to the technique described in [38]. Samples Ts and TsA-I were irradiated by a Co^{60} source with a dose of 10 MRad in air at T = 290 K.

The EPR spectra of lyophilized spin-labeled systems at T = 160 K are characterized by significant broadening of individual components, due to interaction of the nitroxide fragment with the hydroxyl groups of the protein surrounding it.

In Fig. 5, we present the magnetic parameters g_{XX} and A_{ZZ} of radical VIII in spin-labeled cotton fibers, in cellulose, and also in some organic solvents (T = 160 K). The fact that the magnetic parameters of the 5595-V and "Tashkent-I" samples fall on the g_{XX}—A_{ZZ} correlation curve for the model systems makes it logical to assume that the structure and polarity of the microenvironment of radical VIII are identical in the "Tashkent-I" sample and in ethanol, in the 5595-V sample and in a water—glycerin mixture. A different pattern is observed for spin-labeled samples of wilt-contaminated "Tashkent-I" and cellulose. Their magnetic parameters fall outside the general correlation curve. This can be explained by conformational distortions of the radical ring and its microenvironment in these biopolymers.

Upon heating 5595-V cotton fibers and Ts cellulose, we recorded a monotonic shift in the X component of their EPR spectra downfield (Fig. 6). As in the case of lysozyme, this is apparently caused by weakening of the hydrogen bond of the radical fragment with the microenvironment with an increase in temperature.

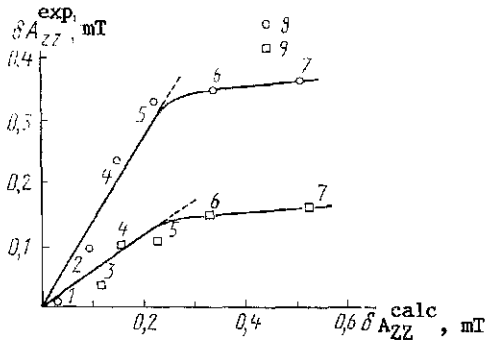

Fig. 8

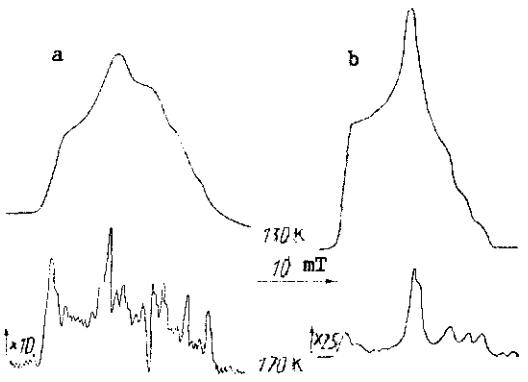

Fig. 9

Fig. 8. Correlation dependences $\delta A_{ZZ}^{exp} - \delta A_{ZZ}^{calc}$ for radicals I (8) and VII (9) in frozen (T = 140 K) toluene (1), isopropanol (2), n-propanol (3), ethanol (4), methanol (5), water–ethanol matrix (3:1) (6), water–glycerin matrix (7).

Fig. 9. Saturation transfer EPR spectra (quadrature components of the second harmonic of the absorption signal) of solutions of radicals IX (a) and X (b) in tert-butylbenzene at temperatures 130 and 170 K.

Starting at a temperature of 315 K, in the EPR spectrum of the 5595-V sample a triplet appears with g = 2.00610 and a = 1.52 mT (Fig. 6a). This can be evidence for the presence in the cotton fibers of amorphous regions in which the label has higher mobility, $\tau_c \approx 2.2 \cdot 10^{-10}$ sec (T = 335 K). The estimate of the fraction of radicals in the amorphous phase (about 2%) is consistent with the value obtained previously in the 3 cm EPR range [34]. The difference between the isotropic g factors of the label found in the crystalline and the amorphous phases of the sample (g_{iso_1} = 2.00553 and g_{iso_2} = 2.00610 respectively) is consistent with the shift of the X component in the EPR spectrum with an increase in temperature downfield and indicates that in amorphous regions of the 5595-V cotton fibers, freezing out of molecular mobility is accompanied by weakening of the hydrogen bond of the radical with its own microenvironment.

In cellulose, we did not note the existence of different phases.

Heating the spin-labeled 5595-V sample up to 335 K leads to a shift in the Z component of its EPR spectrum by 0.7 mT and its broadening by 0.08 mT (Fig. 6a). Such weak broadening of the line with its appreciable shift is not consistent with models of isotropic Brownian rotation and jumps by large angles [34, 39]. This effect can be explained either by compensation narrowing of the line as a result of removal of the inhomogeneous broadening, due to weakening of the hydrogen bond in the radical complex, or by the presence in the system of fast librational vibrations of the radical fragment [40] with frequency $\nu \approx 10^9$ sec^{-1} and amplitude 10 ± 3° (T = 335 K) about the preferred X axis of the radical.

Analysis of relaxation changes in the EPR spectra of cellulose samples (Fig. 6b-d) and the corresponding changes in the theoretically calculated EPR spectra [41] allow us to conclude that Brownian motion of label VIII occurs in the studied systems, with the axis of preferred rotation lying in the XZ plane of the molecular coordinate system. Amorphization of the original sample leads to retardation of the motion of the label in TsA-I and TsA-II (Fig. 6c, d). It is interesting that partial restoration of the elasticity of the microenvironment of the label occurs with a greater degree of amorphization of the sample (Fig. 6d). The activation energy for rotation of radical VIII in samples Ts, TsA-I, TsA-II was 18.4, 43.6, and 29.6 kJ/mole respectively.

The data obtained show that motion of the radical is determined mainly by the form of the cavity "found" by them in the cellulose and the degree of its treatment, which apparently leads to a decrease in the dimensions of this cavity and to a change in the conformation of the rest of the units of the biopolymer.

In order to confirm this hypothesis, we investigated γ-irradiated samples of Ts and TsA-II in the 3 cm and 2 mm EPR ranges.

TABLE 2. Magnetic Parameters of Organic Peroxide Radicals in Model Systems

Radical	Matrix	g_{XX}	g_{YY}	g_{ZZ}	g_{iso}
HOO·	$H_2O_2+H_2O$	2,0329	2,00806	2,00331	2,01478
$(CF_3(CF_2)_x)_2CFOO\cdot$	Free	2,0381	2,00742	2,00231	2,01596
$CF_3(CF_2)_xCF_2OO\cdot$	»	2,0396	2,00770	2,00277	2,01670
$C_6H_{11}OO\cdot$	»	2,0340			
		2,0306	2,00815	2,00279	2,01498
$(C_6H_5)_3COO\cdot$	$(C_6H_5)_3CCl$	2,0310	2,01445	2,00290	2,01612
$(C_6H_5)_2CHOO\cdot$	Free	2,0346	2,00792	2,00212	2,01488
$Br(C_6H_4)C(CH_3)_2OO\cdot$		2,0328			
		2,0228	2,00792	2,00236	2,01436
$(C_6H_5)C(CH_3)_2OO\cdot$	»	2,0334			
		2,0302	2,00824	2,00253	2,01472
$(CH_3)_3COO\cdot$	»	2,0336	2,00830	2,00237	2,01476
$C_2H_5(CH_3)_2COO\cdot$	»	2,0342	2,00859	2,00267	2,01415
$C_3H_7(CH_3)_2COO\cdot$	»	2,0337	2,00801	2,00251	2,01474
$C_3H_7(CH_3)HCOO\cdot$	»	2,0340			
		2,0295	2,00823	2,00240	2,01487
$C_3H_7CH_2OO\cdot$	»	2,0336	2,00816	2,00358	2,01511
$C_2H_5CH_2OO\cdot$	tert-Butylbutyrate	2,0349	2,00792	2,00271	2,01518
$CH_3CONHCHC_3H_7$ (OO·)	Free	2,0323	2,00802	2,00187	2,01408
$CH_3CON(CH_3)CH_2OO\cdot$	»	2,0350	2,00792	2,00180	2,01490
$CH_3CON(C_2H_5)C_2H_4OO\cdot$	»	2,0351			
		2,0309	2,00780	2,00181	2,01489
$CH_3CONHCHCH_3$ (OO·)	»	2,0320	2,00766	2,00339	2,01435

Note. Error in measuring the g_{XX} value is $2\cdot10^{-4}$; for g_{YY} and g_{ZZ} – $3\cdot10^{-5}$. When there is splitting of the X component of the EPR spectrum, in calculation of the g_{iso} value we considered the high-field line. The radicals [except $(CF_3(CF_2)_x)_2CFOO\cdot$, $CF_3\cdot(CF_2)_xCF_2OO\cdot$, $(C_6H_5)_3COO\cdot$ and $C_2H_5CH_2OO\cdot$] were obtained by photolysis of the corresponding hydrogen peroxide at 77 K. The magnetic parameters of the alkyl radicals formed in some systems [53] are not given.

In Fig. 7, we present the EPR spectra of the indicated samples, recorded at T = 290 K in these EPR ranges. Comparison of the EPR spectra for the γ-irradiated original sample Ts (Fig. 7a, b) allows us to conclude that at least three paramagnetic centers with different magnetic parameters are stabilized in it: R_1 is a singlet with g_1 = 2.00281, R_2 is is a doublet with g_2 = 2.00295 and a_2 = 2.9 mT, R_3 is a triplet with g_3 = 2.00442 and a_3 = 2.7 mT. Such an interpretation mainly coincides with that suggested in [35], in which results of mathematical modeling of the EPR spectrum of this sample recorded in the 3 cm EPR range are presented. The presence of the R_1 line can be assigned to residual lignin [35]. Formation of the R_2 and R_3 centers can be explained by the process of dehydration of the glucopyranose ring of the macromolecule at the C_1 and C_4 positions respectively. In TsA-II, upon irradiation at least two more paramagnetic centers (in addition to those listed) are generated (Fig. 7c, d): R_2^* is a doublet with g_2^* = 2.00505 and a_2^* = 1.5 mT, R_3 is a triplet with g_3^* = 2.00532 and a_3^* = 2.2 mT. Formation of these centers in TsA-II can be explained by dehydration of the glucopyranose ring, different from the original conformation, at the C_1 and C_4 positions respectively.

The data obtained make it possible to discuss the question concerning the characteristics of formation of radical complexes in the studied systems.

An important role in complexation of radicals with the environment is played by its structure. Six-membered radicals, in contrast to five-membered radicals having a planar radical ring, are characterized by a chair form of the radical ring. This difference is responsible for the greater accessibility for the partners to their n orbitals and consequently the higher energy of the hydrogen bond with the microenvironment. In fact, the average slope of the g_{XX}–A_{ZZ} correlation curves for the six-membered (I, II) and five-membered (III, VII, VIII) radicals in biological and model systems is $2.3\cdot10^{-3}$ mT^{-1} and $1.2\cdot10^{-3}$ mT^{-1} respectively. This difference indicates a greater shift of spin density to the nitrogen atom upon complexation of the six-membered radicals with the microenvironment [17].

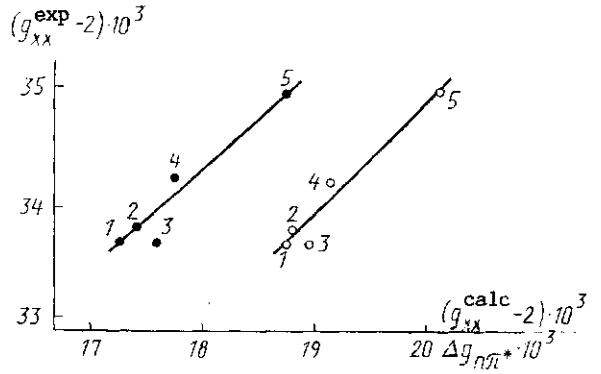

Fig. 10. Correlation curves $g_{XX}^{exp}-g_{XX}^{calc}$ and $g_{XX}^{exp}-\Delta g_{n\pi^*}$ for organic peroxide radicals $C_3H_7CH_2OO\cdot$ (1), $C_3H_7(CH_3)_2COO\cdot$ (2), $(CH_3)_3COO\cdot$ (3), $C_2H_5(CH_3)_2COO\cdot$ (4), $C_2H_5\cdot CH_2OO\cdot$ (5). $\Delta g_{n\pi^*}$ is the shift of the g factor as a result of the $n-\pi^*$ transition.

In biological systems, formation of different types of radical complexes is possible. In Fig. 8, we present the experimentally obtained values of $\delta\Delta_{ZZ}$ and those calculated using formula (2) for the six-membered I and five-membered VII radicals in the model systems. From the figure it is obvious that the linear dependence between the values of δA_{ZZ}^{exp} and δA_{ZZ}^{calc} for both radicals is preserved for a polarity of the microenvironment which is not greater than 1.7 D. This fact indicates the existence in the systems of noncompeting electrostatic and donor–acceptor radical complexes. But the different slope for the curves is evidence for a higher sensitivity of the six-membered radicals to the polarity and structure of the microenvironment.

Thus, in biological and model systems, the magnetic parameters of the radical are determined by the ratio between the complexes formed, and also by the effective polarity and the structure of its microenvironment.

2 mm EPR STUDY OF ANISOTROPIC MOLECULAR ROTATIONS WITH MICROWAVE SATURATION TRANSFER

EPR spectroscopy with microwave saturation transfer considerably expands the range of application of the spin label and spin probe method in the investigation of molecular dynamics in biological and model systems with correlation times $\tau_c \approx 10^{-3}$-10^{-7} sec [5, 42]. However, when recording the saturation transfer EPR spectra in the 3 cm and 8 mm ranges, fundamental difficulties arise in determination of the parameters of anisotropic rotation of the radicals, and also the separation of the effects of motion and magnetic relaxation of the paramagnetic centers [31, 38, 43, 44].

In [45, 46], it was shown to be possible in principle to study ultraslow anisotropic molecular motions of radicals by the saturation transfer EPR method in the 2 mm EPR range.

The saturation transfer EPR spectra, as is well known, are recorded under conditions of microwave saturation and adiabatically fast passage of the system of spin packets. Under these conditions, the change in the spin–lattice relaxation time T_1 and (or) freezing out of rotation of the radical about the preferred axis for some of the spin packets can lead to breakdown of the adiabaticity condition [47]

$$\frac{dH}{dt} \ll \gamma H_1^2 \qquad (4)$$

(here dH/dt is the rate of change of the magnetic field; γ is the gyromagnetic ratio; H_1 is the magnetic component of the microwave oscillations at the sample site) and consequently to removal of the microwave saturation.

Thus, upon rotation of the radical about the molecular X axis, the relative amplitudes of other components of the saturation transfer EPR spectrum decrease. In this case, the

shape of the saturation transfer EPR spectrum will not identically reflect the change in the magnitude of the magnetic relaxation T_1 and the rotational correlation time τ_c of the radical.

The quadrature components of the first harmonic of the dispersion signal and the second harmonic of the absorption signal are the most sensitive to ultraslow anisotropic rotations of spin labels and probes [5, 44].

The EPR and saturation transfer EPR spectra of solutions of radicals IX and X in tert-butylbenzene were recorded in the temperature interval 90-300 K. These radicals are characterized by pronounced anisotropic rotation in the model systems about the X and Y axes respectively.

At temperatures $T \geq 180$ K, the motion of the radicals is anisotropic and occurs with correlation time $\tau_c \leq 10^{-7}$ sec. Extrapolation to the region T = 160 K gave an estimate for their rotational correlation time $\tau_c \simeq 5 \cdot 10^{-7}$ sec. For T < 170 K, the shape of the signals of the first harmonic of the in-phase component of absorption virtually remains unchanged. At the same time, for these temperatures we note an appreciable change in the shape of the saturation transfer EPR spectra of the radicals.

Theoretical calculations [46] have shown that the ratio of intensities of the corresponding components of the second harmonics of the quadrature and in-phase components of the absorption signal is sensitive only to the spin–lattice relaxation time T_1; the ratio of the components of its quadrature saturation transfer EPR spectrum proved to be sensitive to rotation of the radical.

The ratio of the intensities of the X and Y components of the quadrature saturation transfer EPR spectrum of radical IX changes by almost a factor of two in the temperature interval 130-170 K. This is evidence for freezing out its rotation about the X axis with correlation time $\tau_c \simeq 2.8\text{-}4.5 \cdot 10^{-6}$ sec for a change in the spin–lattice relaxation time by a factor of 6-10 (Fig. 9a). In the same temperature interval, in the saturation transfer EPR spectrum of radical X, we recorded more substantial changes (Fig. 9b). An increase in the temperature up to 170 K leads to a change in its rotational correlation time within the range 10^{-5}-10^{-7} sec for an insignificant decrease in the value of T_1 (by a factor of 1.5-2).

Thus, the strongest changes in the saturation transfer EPR spectrum of radical IX are due to the decrease in the spin–lattice relaxation time T_1, and the strongest changes for radical X are due to freezing out ultraslow rotation about its long axis. If the spin–lattice relaxation is determined by the high-frequency, amplitude-restricted motions of the radical, then the rotational mobility is characterized by slower motions with rather high angular amplitude. The differences in the dynamics of radicals IX and X apparently reflect the specifics of their interaction with the environment. Consequently, saturation transfer EPR in the 2 mm range substantially expands the capabilities of the method for study of anisotropic ultraslow molecular motions in different biological systems.

IDENTIFICATION OF PARAMAGNETIC CENTERS FROM THE 2 mm EPR SPECTRA

EPR spectroscopy is widely used to study metabolic and radiation-induced reactions in biological systems [48]. Structural conformational and dynamic properties of the modified systems, and also the biochemical reactions occurring in them, can be determined from analysis of the nature and characteristics of stabilized paramagnetic centers.

In biological systems, the primary radicals are generally centers with localization of the unpaired electron on the carbon and sulfur atoms. In the first case, the g factor of the paramagnetic center usually differs little from the g factor of the free electron. The hyperfine coupling of the unpaired electron with the nearest protons and other nuclei with nonzero spin is easily analyzed from the EPR spectra over a broad registration range [48, 49]. Localization of the unpaired electron on the sulfur atom is responsible for the significant deviation of the g factor of such a center from the pure spin value and its tensor character. The magnetic parameters in this case are also easily determined from the EPR spectra in the standard ranges [50].

Rather frequently peroxide radicals ROO are formed in biological systems as intermediates end products. In these radicals, the unpaired electron is localized mainly on the O–O fragment [51]. This is responsible for the absence of resolved hyperfine structure in the EPR spectra of peroxide radicals and the closeness of their g factors, which makes identification of these centers from the 3 cm EPR spectra significantly more difficult.

In [52], it is shown that the shift in the g factor of peroxide radicals is substantially affected by the donor–acceptor properties of its substituents. The major contribution to this shift comes from the $n-\pi^*$ electronic configuration. It determines the g_{XX} value and to a lesser degree the g_{YY} value of the peroxide radicals. From this it follows that identification of peroxide radicals from their magnetic parameters is possible upon registration of all the components of their EPR spectra. However, the low spectral resolution in the 3 cm EPR range makes it difficult to do this.

As in the case of nitroxide radicals, in the 2 mm EPR range all the components of the EPR spectrum of peroxide radicals are resolved [53]. Furthermore, in this range we can simultaneously register different types of paramagnetic centers formed in condensed media with close g factors. In order to confirm the possibility of identification of peroxide radicals from their magnetic parameters, we compared the experimentally obtained (Table 2) and the theoretically calculated magnetic parameters of some organic peroxide radicals [54].

In Fig. 10, we present the correlation dependences of the experimental and theoretically calculated magnetic parameters of primary and tertiary peroxide radicals (for secondary peroxide radicals, the calculation gives anomalously low values of the magnetic parameters and the eclipsed conformation [54]). From the figure it is obvious that the magnetic parameters of the peroxide radicals substantially depend on the donor–acceptor and conformational properties of their substituents. Therefore, it becomes possible to analyze the structure of the primary and tertiary peroxide radicals in different biological systems from their 2 mm EPR spectra.

Thus, high-resolution EPR spectroscopy allows us to identify different types of paramagnetic centers formed in biological systems with close g factors and to use stable peroxide radicals as spin labels.

From the data presented in this review, it is obvious that high-resolution EPR spectroscopy is an effective tool for solving a broad range of problems in chemical and biological physics. Going to the 2 mm EPR range makes it possible to obtain qualitatively new information in such areas as the metrology of free radicals, spin labels and spin probes, molecular mobility, electronic and spatial structure of paramagnetic centers, local matrix effects, etc. Separate registration of all the components of anisotropic magnetic parameters of different types of paramagnetic centers simplifies and makes possible the analysis of the structural dynamic characteristics of different spin-labeled specimens, including biological systems.

Thus, use of high-resolution EPR spectroscopy combined with spin label and spin probe methods and microwave saturation transfer provides a unique possibility for analysis of fine structural and dynamic transitions in various biological systems.

Further development of high-resolution EPR spectroscopy for more detailed study of biological systems apparently should travel along the path of using pulsed methods with Fourier transformation of the EPR spectra.

I would like to express my sincere thanks to G. I. Likhtenshtein for valuable critical comments, and also Ya. S. Lebedev and O. Ya. Grinberg for discussion of the results.

LITERATURE CITED

1. S. V. Konev, Electronically Excited States of Biopolymers [in Russian], Minsk (1965).
2. V. I. Gol'danskii, Mössbauer Effect and Its Application in Chemistry [in Russian], Moscow (1963).
3. N. A. Kiselev, Electron Microscopy of Biological Molecules [in Russian], Moscow (1965).
4. S. Ohnishi and H. M. McConnell, J. Am. Chem. Soc., 87, No. 9, 2293-2298 (1965).
5. L. Berliner, (ed.), Spin Labeling. Theory and Application, New York (1976), Vol. 1; (1979), Vol. 2.
6. G. I. Likhtenshtein, Spin Label Method in Molecular Biology [in Russian], Moscow (1974).
7. G. I. Likhtenshtein, Polynuclear Oxidation–Reduction Enzymes [in Russian], Moscow (1979).
8. I. V. Dudich, V. P. Timofeev, M. V. Vol'kenshtein, and A. Yu. Misharin, Mol. Biol., 11, 685-689 (1977).
9. V. V. Isaev-Ivanov, V. V. Lavrov, and V. N. Fomichev, Dokl. Akad. Nauk SSSR, 229, No. 1, 70-72 (1976).
10. J. S. Hyde and L. Dalton, Chem. Phys. Lett., 16, No. 1, 568-572 (1972).
11. J. S. Hwang, R. Mason, L. P. Hwang, and J. H. Freed, J. Chem. Phys., 79, No. 2, 489-511 (1975).

12. O. Ya. Grinberg, A. A. Dubinskii, V. F. Shuvalov, et al., Dokl. Akad. Nauk SSSR, 230, No. 4, 884-886 (1976).
13. O. Ya. Grinberg, A. A. Dubinskii, and Ya. S. Lebedev, Usp. Khim., 52, No. 9, 1490-1513 (1983).
14. O. Ya. Grinberg, A. A. Dubinskii, O. G. Poluéktov, and Ya. S. Lebedev, Khim. Fiz., 6, No. 10, 1363-1372 (1987).
15. O. Ya. Grinberg, A. A. Dubinskii, V. N. Krymov, et al., Khim. Fiz., 7, No. 8, 1011-1017 (1988).
16. W. B. Lunch, K. A. Earle, and J. H. Freed, Rev. Sci. Instrum., 59, No. 8, 1345-1351 (1988).
17. A. L. Buchachenko, Complexes of Radicals and Molecular Oxygen with Organic Molecules [in Russian], Moscow (1984).
18. A. Reddoch and S. Konishi, J. Chem. Phys., 70, No. 6, 2121-2128 (1979).
19. A. L. Buchachenko and A. M. Vasserman, Stable Radicals [in Russian], Moscow (1973).
20. E. V. Lyubashevskaya, L. I. Antsiferova, and Ya. S. Lebedev, Teor. Éksp. Khim., 23, No. 1, 46-56 (1987).
21. V. A. Galkin, O. Ya. Grinberg, A. A. Dubinskii, et al., Prib. Tekhn. Éksp., No. 4, 284 (1977).
22. H. A. Kuska and M. T. Rogers, "Electron spin resonance of first row transition metal complex ions," in: Radical Ions, E. T. Kaiser and L. Kevan (eds.), Wiley, New York (1968), pp. 579-745.
23. V. I. Krinichnyi, O. Ya. Grinberg, E. I. Yudanova, et al., Biofiz., 32, No. 2, 215-220 (1987).
24. G. I. Likhtenshtein, Yu. D. Akhmedov, and L. V. Ivanov, Mol. Biol., 8, No. 1, 48-52 (1974).
25. P. O. Schmidt and I. D. Kuntz, Biochem., 23, No. 18, 4261-4265 (1984).
26. V. I. Krinichnyi, O. Ya. Grinberg, V. R. Bogatyrenko, et al., Biofiz., 30, No. 2, 216-219 (1985).
27. G. I. Likhtenshtein, V. R. Bogatyrenko, and A. V. Kulikov, Biofiz., 28, No. 4, 585-589 (1983).
28. V. I. Krinichnyi, O. Ya. Grinberg, E. I. Yudanova, et al., Biofiz., 32, No. 1, 59-63 (1987).
29. O. H. Griffith and P. Jost, The Spin Label Method. Theory and Application [Russian translation], Moscow (1979), pp. 516-524.
30. J. H. Fendler and E. J. Fendler, Catalysis in Micellar and Macromolecular Systems, New York (1975).
31. O. V. Belonogova, G. I. Likhtenshtein, A. V. Levashov, et al., Biokhim., 48, No. 3, 379-386 (1983).
32. F. M. Menger, G. Saito, G. V. Sanzero, and J. R. Dodd, J. Am. Chem. Soc., 97, No. 4, 909-911 (1975).
33. V. I. Krinichnyi, Dissertation in competition for the academic degree of Candidate of the Physical/Mathematical Sciences, Chernogolovka (1986).
34. I. Kh. Yusupov, P. Kh. Bobodzhanov, R. Marupov, et al., Vysokomolek. Soedin., A26, No. 2, 369-373 (1984).
35. B. G. Ershov and A. S. Klimentov, Usp. Khim., 53, No. 12, 2056-2059 (1984).
36. V. I. Krinichnyi, O. Ya. Grinberg, I. Kh. Yusupov, et al., Biofiz., 31, No. 3, 482-485 (1986).
37. V. I. Krinichnyi and N. V. Kostina, Abstracts: International Conference on Nitroxide Radicals [in Russian], Novosibirsk (1989), p. 63.
38. R. Marupov, P. Kh. Bobodzhanov, I. Kh. Yusupov, et al., Biofiz., 24, No. 3, 519-523 (1979).
39. O. G. Poluéktov, E. V. Lyubashevskaya, A. A. Dubinskii, et al., Khim. Fiz., 4, No. 12, 1615-1618 (1985).
40. M. E. Johnson, Biochem., 17, No. 7, 1223-1228 (1978).
41. L. I. Antsiferova and E. A. Lyubashevskaya, Atlas of EPR Spectra of Nitroxide Radicals in the 2 mm Range [in Russian], Chernogolovka (1986).
42. M. A. Hemminga, Chem. Phys. Lipids, 32, No. 1, 323-383 (1983).
43. B. H. Robinson and L. R. Dalton, J. Chem. Phys., 72, No. 4, 1312-1323 (1980).
44. M. E. Johnson and L. Lie, Biochem., 21, No. 23, 4459-4463 (1982).
45. Ya. S. Lebedev, L. I. Antsiferova, O. Ya. Grinberg, et al., Second Conference on Modern Methods of RF Spectroscopy, DDR-8804 (1985), pp. 48-57.
46. V. I. Krinichyi, O. Ya. Grinberg, A. A. Dubinskii, et al., Biofiz., 32, No. 3, 534-535 (1987).

47. A. A. Bugai, Fiz. Tverd. Tela, 4, No. 11, 3027-3034 (1962).
48. D. J. E. Ingram, Biological and Biochemical Applications of Electron Spin Resonance, Hilger, London (1969).
49. H. K. Roth, F. Keller, and H. Schneider, High-Frequency Spectroscopy in Polymer Research [Russian translation], Moscow (1987).
50. W. Gordy and Y. Kurita, J. Chem. Phys., 34, No. 1, 282-288 (1960).
51. D. C. H. McBrein and T. F. Slater, Free Radicals, Lipid Peroxidation and Cancerogens, London (1982).
52. D. C. McCain and W. E. Palke, J. Magn. Reson., 20, No. 1, 52-66 (1975).
53. V. I. Krinichnyi, V. F. Shuvalov, O. Ya. Grinberg, and Ya. S. Lebedev, Khim. Fiz., No. 5, 621-627 (1983).
54. A. F. Dmitruk, L. I. Kholoimova, V. I. Krinichnyi, et al., Khim. Fiz., 5, No. 4, 479-483 (1986).

APPLICATION OF THE METHOD OF MODULATING THE REABSORPTION FOR INVESTIGATIONS OF THE PLASMA OF METAL VAPOR LASERS

A. N. Mal'tsev

UDC 533.9:621.378.826

The author of [1] has described a method of determining the populations of energy levels from measured modulation coefficients β_{ik} of the intensities of a few spectral lines under conditions of partial reabsorption; a graphic method of solving the respective systems of nonlinear algebraic equations was used. We consider here the solution of test problems which outline the possible use of the method for the determination of populations N_i, N_k of operational levels under the typical conditions of gas laser operation. At the present time investigations of a possible further increase in the efficiency of generation is one of the most important problems in the physics of gas lasers; the efficiency is given, first of all, by the efficiency of pumping the operational levels, i.e., their populations under various conditions. Lasers based on self-limited transitions in metal vapors are characterized by the most efficient generation in the visible and near-infrared parts of the spectrum [2]. To be more specific, we will consider the possibilities of determining the populations of the operational levels in the most powerful of the metal-vapor lasers, namely in copper vapor lasers.

The main feature of employing tghe modulation of the reabsorption in non-stationary discharges, including copper vapor lasers, must be noted. This feature is related to the fact that the rate of change of the measured population levels as a function of time must not be too large because a photon carrying information on the quantity $N_i S(\varkappa_{ik} L)$ must have time to fly out of the object under investigation until N_i, $\varkappa_{ik}$ will have changed substantially. $\varkappa_{ik}$ denotes the absorption coefficient in an $i \to k$ transition and S denotes the reabsorption function. In this case the condition of a quasi-stationary dependence of the reabsorption function upon its arguments will be satisfied; generally speaking, this condition is imposed in any method of measuring populations from the intensity of spectral lines which are partially reabsorbed. In the case of resonance lines, we usually assume for the population of the ground state $N_0(t) \approx \text{const}$ [1] and $\varkappa_{i0} \sim N_0 \approx \text{const}$, i.e., we assume that $S(\varkappa_{i0} L)$ is essentially stationary.

The condition of a stationary $S(\varkappa_{ik} L)$ means for partially reabsorbed lined that the effective time constant τ_N of the change of the populations under consideration must be much larger than the time $\tau_{ph} = L/c$ required by the photon for flying through the volume examined in the direction of the change. The length τ_s of the measurement strobe obviously must not exceed the order of magnitude of τ_{ph}. Thus, the inequality $\tau_s \lesssim \tau_{ph} \ll \tau_N \lesssim \Delta\tau$ must be satisfied, where $\Delta\tau$ denotes the time interval between two ensuing population measurements.

The following values of these quantities are characteristic of lasers working with copper vapors: $L \sim 0.3$-1 m; $\tau_{ph} \sim 1$-3 nsec; $\tau_N \gtrsim 20$-30 nsec [3, 4]. Consequently, $\tau_s \lesssim 1$ nsec and $\Delta\tau \gtrsim 20$-30 nsec. These conditions can be easily met in an experiment.

Institute of Atmospheric Optics, Siberian Branch, Academy of Sciences of the USSR, Tomsk.
Translated from Zhurnal Prikladnoi Spektroskopii, Vol. 52, No. 6, pp. 906-912, June, 1990. Original article submitted May 10, 1989.

0021-9037/90/5206-0591$12.50